Sinusoidal electromagnon in $R\mathrm{MnO}_3$: Indication of anomalous magnetoelectric coupling

Markku P. V. Stenberg[1,2,*] and Rogério de Sousa[1,†]

[1]*Department of Physics and Astronomy, University of Victoria, Victoria, B.C., V8W 3P6, Canada*
[2]*Department of Microelectronics and Nanoscience, Chalmers University of Technology, S-41296 Göteborg, Sweden*

(Dated: November 8, 2011)

The optical spectra in the family of multiferroic manganites $R\mathrm{MnO}_3$ is a great puzzle. Current models can not explain the fact that two strong electromagnons are present in the non-collinear spin cycloidal phase, with only one electromagnon surviving the transition into the collinear spin sinusoidal phase. We show that this is a signature of the presence of anomalous magnetoelectric coupling that breaks rotational invariance in spin space and generates oscillatory polarization in the ground state.

PACS numbers: 75.80.+q, 78.20.Ls, 71.70.Ej, 75.30.Et

I. INTRODUCTION

In multiferroic materials magnetic and electric orders coexist simultaneously and the coupling between spin and charge degrees of freedom gives rise to a wide range of magnetoelectric phenomena[1–3]. Recent research has centered on the origin and symmetry of magnetoelectric coupling. The crucial question is how the coupling between two spins depends on electric field:

$$H_{\mathrm{me}} = \sum_{nm} \Big[J_{nm}(\mathbf{E})\hat{\mathbf{S}}_n \cdot \hat{\mathbf{S}}_m + \mathbf{D}_{nm}(\mathbf{E}) \cdot \hat{\mathbf{S}}_n \times \hat{\mathbf{S}}_m + \hat{\mathbf{S}}_n \cdot \mathbf{A}_{nm}(\mathbf{E}) \cdot \hat{\mathbf{S}}_m \Big]. \quad (1)$$

Here $\hat{\mathbf{S}}_n$ and $\hat{\mathbf{S}}_m$ are spins at lattice sites $\mathbf{R}_n$ and $\mathbf{R}_m$, and the electric field $\mathbf{E}$ can be either internal, i.e., from the electric polarization in the material, or external, as is the case of incident light. The first two interactions in the right hand side of Eq. (1) are well understood. The first one, exchange interaction J, is electric-field dependent because atomic positions are modulated by $\mathbf{E}$ (the phenomena of magnetostriction). The second one, the Dzyaloshinskii-Moriya (DM) interaction, is first order in spin-orbit coupling and is antisymmetric under spin interchange. The third and final interaction, the anomalous tensor $\mathbf{A}$, is instead symmetric under spin interchange; it is known to originate from second order spin-orbit effects[4], but is usually believed to be weak or hard to probe. Nevertheless, its electric field dependence has not been studied.

Most interesting effects take place when one of the coupling coefficients depends *linearly* on electric field. For instance, simple models based on electronic[5] or lattice mediated polarization[6] predict that the DM vector is electric-field dependent according to $\boldsymbol{D}_{nm} \propto \mathbf{E} \times (\mathbf{R}_n - \mathbf{R}_m)$; this gives rise to the phenomena of magnetically induced ferroelectricity observed in a large class of materials, the cycloidal multiferroics[5–8].

In addition, the linear magnetoelectric effect makes magnetic excitations electrically dipole active. This gives rise to the electromagnon, the quasiparticle of the multiferroic state[9–18]. The observation of electromagnons in optical experiments provide invaluable clues on the symmetry and magnitude of the magnetoelectric coupling present in Eq. (1). Moreover, the ability to launch, detect, and control magnons electrically also holds promise for novel applications in information processing[19,20].

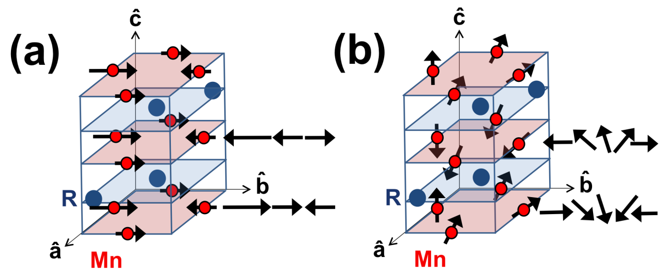

FIG. 1: (Color online) Schematics of low temperature phases of $R\mathrm{MnO}_3$: (a) Collinear sinusoidal phase and (b) Non-collinear cycloidal phase.

The observation of magnetically-induced ferroelectricity[8] and electromagnons[10] in the class of perovskite manganites $R\mathrm{MnO}_3$ has made this material the prototype for studies of strong magnetoelectric effects. Here R is a rare-earth ion such as Dy, Tb, Gd or their mixture, *e.g.*, $\mathrm{Gd}_x\mathrm{Tb}_{1-x}$. In the $R\mathrm{MnO}_3$ family, spins are typically ordered with a period incommensurate with the lattice[8,14]. Below the first Néel temperature ($T = 39$ K in DyMnO_3), the ground state of the Mn spins forms the collinear sinusoidal density wave depicted in Fig. 1(a). At even lower temperature (19 K in DyMnO_3), another phase transition takes place where the Mn spins order non-collinearly in the cycloid ground state shown in Fig. 1(b).

The detection of electromagnons in the cycloidal phase of $R\mathrm{MnO}_3$ led to a surprising observation. Optical experiments showed that two quite strong electromagnons are observed in the cycloidal phase, provided the electric field of light was directed along the crystallographic

direction $\hat{\mathbf{a}}$[13,15,21]. This remained true even when the cycloid plane was flipped, leading to the conclusion that the DM interaction $\mathbf{D}$ could not explain the origin of the observed strong electromagnon resonances (but in recent experiments a weak electromagnon resonance consistent with the DM model was observed[22]). This is a surprising conclusion in view of the fact that the DM interaction is known to be responsible for ferroelectricity in these materials.

Optical experiments have also produced a puzzling observation: *The lower energy electromagnon, unlike the higher energy one, survives also in the collinear sinusoidal phase.* This is observed, e.g., in $DyMnO_3$[21], $Gd_{0.7}Tb_{0.3}MnO_3$[23], and $Eu_{1-x}Y_xMnO_3$[24], but in $TbMnO_3$ no electromagnons are discernible in the sinusoidal phase[12].

Currently, there exists a consensus that the high energy electromagnon originates from magnetostriction, the first term in Eq. (1)[13,16,17]. However, no consensus exists on the origin of the low energy electromagnon. Two quite different models were proposed for its explanation: In [16], we showed that magnetostriction plus spin-orbit coupling is able to explain the origin of both electromagnons even when the cycloid ground state is purely harmonic. In [17], Mochizuki *et al.* showed that pure magnetostriction plus cycloid anharmonicity (without a tensor $\mathbf{A}$) is able to explain the two electromagnons of the cycloid phase, suggesting that anharmonicity plays a vital role (similar results for $BiFeO_3$ were proposed in [25]). *But neither of the two above-mentioned models is able to explain the optical activity of the low energy electromagnon in the sinusoidal phase.*

II. MODEL FOR $R\mathrm{MnO}_3$

Here we present a model of electromagnon excitations that can explain the optical experiments in both the sinusoidal and in the cycloidal phases. Our model Hamiltonian consists of spin and phonon couplings, $H = H_S + H_{\rm ph} + H^{(1)}_{\rm me} + H^{(2)}_{\rm me}$. Here H_S describes exchange interactions and single-ion anisotropies,

$$H_S = \sum_{n,m} J_{n,m} \hat{\mathbf{S}}_n \cdot \hat{\mathbf{S}}_m + D_a \sum_n (\hat{\mathbf{S}}_n \cdot \hat{\mathbf{a}})^2 - D_b \sum_n (\hat{\mathbf{S}}_n \cdot \hat{\mathbf{b}})^2. \tag{2}$$

We assume $D_a > 0$ and $D_b > 0$, favoring alignment along the $\hat{\mathbf{b}}$ direction. The spins are coupled by exchange interactions $J_{n,m}$, with nearest-neighbor interactions in the ab plane denoted by J_0, next-nearest-neighbor interaction along $\hat{\mathbf{b}}$ denoted by J_{2b}, and interaction along the $\hat{\mathbf{c}}$ direction denoted by J_c. The interaction $J_0 < 0$ is ferromagnetic while $J_{2b} > 0$ and $J_c > 0$ are both antiferromagnetic.

At sufficiently low temperatures, provided that the stability condition $J_{2b} > -J_0/2$ is satisfied, the competition between the nearest-neighbor ferromagnetic exchange, and the antiferromagnetic next-nearest-neighbor exchange favors incommensurate spin ordering. Between the first and second Néel temperatures the spins order in a sinusoidal density wave,

$$\boldsymbol{S}_0(\mathbf{R}, T) = \pm S(T) \cos(\mathbf{Q} \cdot \mathbf{R} + \phi) \hat{\mathbf{b}}, \tag{3}$$

with $S(T)$ a temperature dependent amplitude [see Eq. (3.14) in Ref. 26 for its dependence on model parameters]. The magnitude of the sinusoidal wave vector Q is given by $\cos(Qb/2) = -J_0/(2J_{2b})$. The upper sign in Eq. (3) corresponds to ab layer spins with the integer c-coordinate, while the lower sign applies to spins in the neighboring ab layers a distance $c/2$ above and below them.

Our phonon Hamiltonian is

$$H_{\rm ph} = \frac{1}{2} m^* \sum_n \left(\dot{\boldsymbol{x}}_n^2 + \omega_0^2 \boldsymbol{x}_n^2 \right) - e^* \sum_n \boldsymbol{x}_n \cdot \boldsymbol{E}, \tag{4}$$

where ω_0 is the (bare) phonon frequency, m^* is the effective mass, $\boldsymbol{x}_n$ is the relative displacement between anions and cations in the nth unit cell, e^* is the Born charge, and $\boldsymbol{E}$ is the electric field of light.

We divide the linear magnetoelectric couplings in our model into two separate terms, $H^{(1)}_{me}$ and $H^{(2)}_{me}$. The first interaction,

$$\begin{aligned} H^{(1)}_{\rm me} \;=\; & e^* \sum_n x_n^a [g_c(\hat{S}^c_{1,n} - \hat{S}^c_{1,n+b})(\hat{S}^c_{2,n} + \hat{S}^c_{2,n+a}) \\ & + g_b(\hat{S}^b_{1,n} - \hat{S}^b_{1,n+b})(\hat{S}^b_{2,n} + \hat{S}^b_{2,n+a}) \\ & + (1 \to 3, 2 \to 4)], \end{aligned} \tag{5}$$

does not give rise to electromagnons in a collinear ground state, but is necessary to explain the origin of the low frequency electromagnon in the cycloidal phase[16]. The second interaction is instead given by

$$\begin{aligned} H^{(2)}_{\rm me} \;=\; & e^* \sum_n x_n^a \{ [g_{bc}(\hat{S}^b_{1,n} - \hat{S}^b_{1,n+b})(\hat{S}^c_{2,n} + \hat{S}^c_{2,n+a}) \\ & + g_{ab}(\hat{S}^a_{1,n} - \hat{S}^a_{1,n+b})(\hat{S}^b_{2,n} + \hat{S}^b_{2,n+a}) + (1 \leftrightarrow 2)] \\ & + (1 \to 3, 2 \to 4)\}, \end{aligned} \tag{6}$$

where g_{ab} and g_{bc} are coupling constants that can be obtained by microscopic calculation (e.g., using density functional theory). Like Eq. (5), this spin-symmetric interaction is also invariant under the $Pbnm$ space-group operations of $R\mathrm{MnO}_3$, and is therefore consistent with lattice symmetry. Both interactions represent anomalous magnetoelectric coupling, with particular forms of the anomalous tensor $\boldsymbol{A}$ [Eq. (1)]. A generalization of Moriya's theory[4] to allow for magnetostriction effects shows that such interactions can originate from cross-coupling between spin-orbit and magnetostriction effects. However, a full microscopic theory is still needed to confirm this expectation.

III. ELECTROMAGNON SPECTRA

We adopt the molecular field approximation and expand the Hamiltonian H by keeping only terms quadratic

in the fluctuation operators, e.g., $\delta\hat{S}_c^2$, $\delta\hat{S}_a\delta P_a$, δP_a^2, etc. We parametrize the spin excitations $\delta\hat{\boldsymbol{S}} = \hat{\boldsymbol{S}} - \boldsymbol{S}_0$ by $\delta\hat{\boldsymbol{S}}_{i,n} = \hat{s}^a_{i,n}\hat{\mathbf{a}} \pm \hat{s}^c_{i,n}\hat{\mathbf{c}}$, and compute the equations of motion using the canonical commutation relations, $[\hat{s}^c_{j,n}, \hat{s}^a_{k,m}] = i\delta_{jk}\delta_{nm}\hat{S}^b_k$. In addition, we also adopted the random phase approximation (RPA), i.e., we made the substitution $\hat{S}^b_k \to \langle\hat{S}^b_k\rangle = \boldsymbol{S}_0(\boldsymbol{R}_k, T)\cdot\hat{b}$ in the commutator above. Such an approximation is expected to hold when the fluctuation effects are not too large (i.e., we are sufficiently far from the Néel temperature).

After some manipulation the coupled equations of motion for spins and polarization is given by,

$$\left(\omega^2 - \Omega^2_{\mathrm{C,q}}\right)\left(s^\alpha_{1q} + s^\alpha_{2q} + s^\alpha_{3q} + s^\alpha_{4q}\right) = \Omega_{\mathrm{C,q}}\Gamma_q, \quad \text{(7a)}$$

$$\left(\omega^2 - \Omega^2_{\mathrm{C,q+k_0}}\right)\left(s^\alpha_{1q} - s^\alpha_{2q} + s^\alpha_{3q} - s^\alpha_{4q}\right) = \Omega_{\mathrm{C,q+k_0}}\Gamma_{q+k_0}, \quad \text{(7b)}$$

$$\left(\omega^2 - \Omega^2_{\mathrm{EC,q}}\right)\left(s^\alpha_{1q} + s^\alpha_{2q} - s^\alpha_{3q} - s^\alpha_{4q}\right) = 0, \quad \text{(7c)}$$

$$\left(\omega^2 - \Omega^2_{\mathrm{EC,q+k_0}}\right)\left(s^\alpha_{1q} - s^\alpha_{2q} - s^\alpha_{3q} + s^\alpha_{4q}\right) = 0, \quad \text{(7d)}$$

where $\alpha = a, c$. Here s^α_{iq} is the momentum representation of the spin fluctuation s^α_{in}. Equations (7a) and (7b) are related by a shift in momentum space, $\boldsymbol{q} \leftrightarrow \boldsymbol{q} + \boldsymbol{k}_0$ where $k_0 = 2\pi/b$ is the Brillouin zone-edge for magnons. Such a relationship corresponds to the fact that "anti-phase" fluctuations of neighboring spins with wave vector q are equivalent to "in-phase" fluctuations at $q + 2\pi/b$. They describe a mode here referred to as a cyclon, with dispersion $\Omega_{C,q}$. Similarly, Eqs. (7c) and (7d) share the same momentum shift relationship, but describe a different mode referred to as an extra-cyclon. The cyclon and extra-cyclon dispersions are shown in Fig. 2. We note that the cyclon has a gap proportional to D_b, while the extra-cyclon has a gap proportional to $(2J_c + D_b)$.

Equations (7a) and (7b) show that $H^{(2)}_{me}$ couples only a single electromagnon, the cyclon at $q = k_0 - 2Q$, to the polar phonon. This takes place through dynamic magnetoelectric coupling $\Omega_{\mathrm{C,q}}\Gamma_q$ with

$$\Gamma_q = \Gamma^{ab}_q - \Gamma^{bc}_q, \quad \Gamma^{bc}_q = \Gamma^{ab}_q(g_{ab} \to g_{bc}), \quad (8)$$

$$\Gamma^{ab}_q = \frac{g_{ab}S(T)^2 v_0 \sin\left(\frac{Qb}{2}\right)\delta P^a_0}{\hbar}\left[e^{-2i\phi}\delta_{q-k_0+2Q} - e^{2i\phi}\delta_{q-k_0-2Q} + e^{-2i\phi}\delta_{q+k_0+2Q} - e^{2i\phi}\delta_{q+k_0-2Q}\right]. \quad (9)$$

Optical experiments such as transmissivity or reflectivity probe the frequency dependence of the dielectric function $\epsilon(\omega)$. After a linear response calculation we obtain

$$\varepsilon(\omega) = \frac{\mathcal{S}_{em}}{\Omega^2_{C,k_0-2Q} - \Delta^2 - \omega^2} + \frac{\mathcal{S}_{ph}}{\omega_0^2 + \Delta^2 - \omega^2} + \varepsilon_\infty. \quad (10)$$

Hence $\epsilon(\omega)$ can be written as two Lorentzians, with poles at downshifted magnon and upshifted phonon frequencies. The pole at the magnon frequency shows that the cyclon at $q = k_0 - 2Q$ is actually an electromagnon, with spectral weight given by

$$\mathcal{S}_{em} = \frac{4\pi\chi_0\omega_0^2\Delta^2}{\omega_0^2 - \Omega^2_{C,k_0-2Q}}. \quad (11)$$

Here $\chi_0 = e^{*2}/(m^* v_0 \omega_0^2)$ is the zero-frequency susceptibility, with v_0 the unit cell volume. The frequency shift Δ is calculated to be

$$\Delta^2 \approx \frac{S(T)^2 e^{*2}(g_{bc} - g_{ab})^2 \tan^2\left(\frac{Qb}{2}\right)\Omega^2_{C,k_0-2Q}}{2m^*(\omega_0^2 - \Omega^2_{C,k_0-2Q})\left[\sin^4\left(\frac{Qb}{2}\right) + \cos^4\left(\frac{Qb}{2}\right)\right]J_{2b}}, \quad (12)$$

apart from smaller terms of order $(g_{ab} - g_{bc})g_{ab}$. Since the magnitude of the frequency shift Δ is the same for the magnon and the phonon, we confirm the oscillator strength sum rule $\mathcal{S}_{em} + \mathcal{S}_{ph} = 4\pi\chi_0\omega_0^2$.

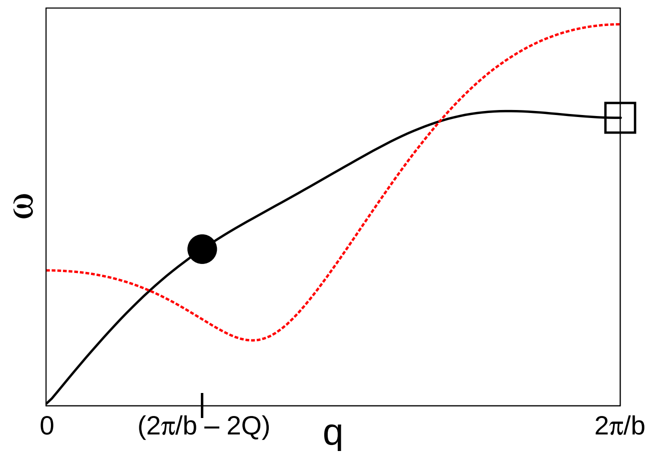

FIG. 2: (Color online) Typical dispersion curves for magnon wavevector $\mathbf{q}$ along $\hat{\mathbf{b}}$ in the sinusoidal phase: cyclon (black solid) and extra-cyclon (red dashed). In the sinusoidal state, only the low-energy electromagnon (filled circle) is activated, through $H^{(2)}_{me}$ [Eq. (6)]. In the cycloidal state, $H^{(1)}_{me}$ [Eq. (5)] activates also the zone-edge electromagnon (hollow square).

IV. ADDITIONAL CONSEQUENCE OF ANOMALOUS MAGNETOELECTRIC INTERACTION: INCOMMENSURATE OSCILLATORY POLARIZATION

In addition to the sinusoidal electromagnon, the couplings described by Eqs. (5) and (6) have an important observational consequence: They lead to an incommensurate oscillatory polarization (IOP) with wavevector $2Q$[16]. Minimizing Eqs. (4)–(6) with respect to the polar phonon displacement $\mathbf{x}_n$ and plugging in the cycloidal spin order

	Electromagnons (Far-IR)	Atomic disp. (X-ray)
Cycloidal	$(g_b + g_c)$	$(g_b - g_c)$
	$(g_b - g_c)$	g_{bc}
Sinusoidal	$(g_{bc} - g_{ab})g_{ab}$	g_b

TABLE I: This table relates our predictions for optical and X-ray experiments to the anomalous magnetoelectric coupling parameters g_α and $g_{\alpha\beta}$ introduced in this paper ($\alpha, \beta = a, b, c$ are crystallographic directions). The first column refers to measurements of electromagnon spectral weight using far-IR optical experiments, and the second column refers to the measurement of magnetically induced lattice distortions using X-ray spectroscopy. Each experiment has different magnetoelectric signatures, depending on whether the ground state is cycloidal or sinusoidal. All parameters can be measured individually, and in addition, parameters g_b and g_c can be cross-checked.

we get

$$\frac{e^*\mathbf{x}_n}{v_0} = 4\chi_0 S^2 \sin\left(\frac{Qb}{2}\right)\{(g_b - g_c)\sin[Qb(2n+1)] - g_{bc}\cos[Qb(2n+1)] + g_{bc}\}\,\hat{\mathbf{a}}. \quad (13)$$

Note how g_{bc} generates a combination of static and oscillatory polarization along the $\hat{\mathbf{a}}$ direction.

When the system goes into the sinusoidal phase, this polarization changes discontinously to

$$\frac{e^*\mathbf{x}_n}{v_0} = 4\chi_0 S(T)^2 \sin\left(\frac{Qb}{2}\right) g_b \sin[(2n+1)Qb]\hat{\mathbf{a}}. \quad (14)$$

Such an oscillatory polarization can be detected by X-ray scattering. Indeed, Kimura *et al.* detected an oxygen oscillation with wavevector $2Q$ in both the cycloidal and sinusoidal phases [see blue dots in Fig. 1(c) of [8]]. Just like our prediction, the X-ray intensity in [8] showed an apparent discontinuity in oxygen displacements in the transition from cycloidal to sinusoidal phase.

Table I shows how a combination of optical and X-ray scattering experiments are capable of measuring the magnetoelectric coupling constants individually, and even cross-check some of them. For instance, for $DyMnO_3$, we obtain from the measured electromagnon spectral weights[21] and X-ray diffraction intensities[27] in the sinusoidal and cycloidal phases the values of $g_b \sim 170$ erg/(cm esu), $g_c \sim -40$ erg/(cm esu), $g_{ab} \sim 100$ erg/(cm esu) $\gg g_{bc}$. In $TbMnO_3$, the sinusoidal electromagnon could not be observed experimentally[12]. This indicates that $g_{ab}, g_{bc} \ll g_b, g_c$, i.e., $H^{(2)}_{\rm me}$ is much weaker than $H^{(1)}_{\rm me}$ in $TbMnO_3$.

V. DISCUSSION AND CONCLUSION

We now consider the justification of our model and other possibilities for the activation of the electromagnon in the collinear sinusoidal phase. First, we note that the presence of DM interaction in principle also predicts an electromagnon in the collinear sinusoidal state[28,29]. However, this scenario is ruled out by the experiments where the electromagnon is activated with $\boldsymbol{E}$ along $\hat{\boldsymbol{a}}$ only. In addition to the DM interaction, there are no other linear magnetoelectric couplings anti-symmetric under the exchange of spins that would be allowed by lattice symmetry.

The anharmonic cycloid model of Mochizuki *et al.*[17] would give rise to no electromagnon activity in the sinusoidal phase. One possibility for the activation of sinusoidal electromagnons in this scenario would be to include additional single-ion anisotropy so that the spins in the ground state are tilted off the $\hat{b}$ axis[30]. However, in this case *both high and low energy electromagnons get activated*. We found no scenario where deformation of the sinusoidal ground state activates the low-energy electromagnon without activating the high-energy one.

Concerning other possible symmetry-allowed magnetoelectric interactions, we note that the other couplings quadratic in spin do not couple electric field linearly to magnons. More specifically, terms of the form $x^a_n S^a_i S^a_j$, $x^a_n S^c_i S^c_j$, and $x^a_n S^a_i S^c_j$ lead to contributions that are third order in fluctuation operators, and the term $x^a_n S^b_i S^b_j$ does not couple polarization to magnons. Hence in the collinear sinusoidal state only the couplings linear in S^b considered in the present work [Eq. (6)] can be responsible for the electromagnons in collinear sinusoidal state.

In conclusion, we showed that anomalous magnetoelectric coupling gives a natural explanation for the origin of electromagnons in both the cycloidal and sinusoidal phases of RMnO$_3$. It remains an open question to study, e.g., through ab-initio methods, the microscopic mechanism of anomalous magnetoelectric coupling.

We acknowledge support from NSERC discovery.

* markku.stenberg@iki.fi
† rdesousa@uvic.ca

1 W. Eerenstein, N. D. Mathur, and J. F. Scott, Nature **442**, 759 (2006).
2 Y. Tokura, Science **312**, 1481 (2006).
3 S.-W. Cheong and M. Mostovoy, Nature Mater. **6**, 13 (2007).
4 T. Moriya, Phys. Rev. **120**, 91 (1960).
5 H. Katsura, N. Nagaosa, and A.V. Balatsky, Phys. Rev. Lett. **95**, 057205 (2005).
6 I. A. Sergienko and E. Dagotto, Phys. Rev. B **73**, 094434 (2006).
7 M. Mostovoy, Phys. Rev. Lett. **96**, 067601 (2006).
8 T. Kimura, T. Goto, H. Shintani, K. Ishizaka, T. Arima, and Y. Tokura, Nature **426**, 55 (2003).
9 V.G. Bar'yakhtar and I.E. Chupis, Sov. Phys. Solid State

10, 2818 (1969).
[10] A. Pimenov, A. A. Mukhin, V. Y. Ivanov, V. D. Travkin, A. M. Balbashov, and A. Loidl, Nature Phys. **2**, 97 (2006).
[11] H. Katsura, A. V. Balatsky, and N. Nagaosa, Phys. Rev. Lett. **98**, 027203 (2007).
[12] Y. Takahashi, N. Kida, Y. Yamasaki, J. Fujioka, T. Arima, R. Shimano, S. Miyahara, M. Mochizuki, N. Furukawa, and Y. Tokura, Phys. Rev. Lett. **101**, 187201 (2008).
[13] R. Valdés Aguilar, M. Mostovoy, A. B. Sushkov, C. L. Zhang, Y. J. Choi, S-W. Cheong, and H. D. Drew, Phys. Rev. Lett. **102**, 047203 (2009).
[14] N. Kida *et al.*, J. Opt. Soc. Am. B **26**, A35 (2009).
[15] J.S. Lee, N. Kida, S. Miyahara, Y. Takahashi, Y. Yamasaki, R. Shimano, N. Furukawa, and Y. Tokura, Phys. Rev. B **79**, 180403(R) (2009).
[16] M. P. V. Stenberg and R. de Sousa, Phys. Rev. B **80**, 094419 (2009).
[17] M. Mochizuki, N. Furukawa, and N. Nagaosa, Phys. Rev. Lett. **104**, 177206 (2010).
[18] P. Rovillain, M. Cazayous, Y. Gallais, M-A. Measson, A. Sacuto, H. Sakata, and M. Mochizuki, Phys. Rev. Lett. **107**, 027202 (2011).
[19] R. de Sousa and J. E. Moore, Appl. Phys. Lett. **92**, 022514 (2008).
[20] P. Rovillain, R. de Sousa, Y. Gallais, A. Sacuto, M.A. Measson, D. Colson, A. Forget, M. Bibes, A. Barthélémy, and M. Cazayous, Nature Materials **9**, 975 (2010).
[21] N. Kida, Y. Ikebe, Y. Takahashi, J. P. He, Y. Kaneko, Y. Yamasaki, R. Shimano, T. Arima, N. Nagaosa, and Y. Tokura, Phys. Rev. B **78**, 104414 (2008).
[22] A. M. Shuvaev, V. D. Travkin, V. Y. Ivanov, A. A. Mukhin, and A. Pimenov, Phys. Rev. Lett. **104**, 097202 (2010).
[23] N. Kida *et al.*, J. Phys. Soc. Jpn. **77**, 123704 (2008).
[24] Y. Takahashi, Y. Yamasaki, N. Kida, Y. Kaneko, T. Arima, R. Shimano, and Y. Tokura, Phys. Rev. B **79**, 214431 (2009).
[25] R. de Sousa and J. E. Moore, Phys. Rev. B **77**, 012406 (2008).
[26] T. Nagamiya, Solid State Physics **20**, 305 (1967).
[27] T. Kimura, S. Ishihara, H. Shintani, T. Arima, K. T. Takahashi, K. Ishizaka, and Y. Tokura, Phys. Rev. B **68**, 060403 (2003).
[28] I. E. Chupis, Low Temp. Phys. **33**, 715 (2007).
[29] D. Senff *et al.*, J. Phys. Condens. Matter **20**, 434212 (2008).
[30] M. Mochizuki and N. Furukawa, Phys. Rev. B **80**, 134416 (2009).